Int. J. Electrochem. Sci., 10 **(2015)** 8941 - 8950

International Journal of
ELECTROCHEMICAL
SCIENCE
www.electrochemsci.org

Short Communication

Thermal Insitu Analyses of Multicomponent Pyrophosphate Cathodes Materials

R. A. Shakoor[1,*], *Ramazan Kahraman*[2,*], *Arsalan A. Raja*[2]

[1] Center for Advanced Materials (CAM), Qatar University, 2713, Doha, Qatar
[2] Department of Chemical Engineering, Qatar University, 2713, Doha, Qatar
[*]E-mail: Shakoor@qu.edu.qa, ramazank@qu.edu.qa

Received: 10 August 2015 / *Accepted:* 15 September 2015 / *Published:* 30 September 2015

Development of secondary batteries based on abundant and inexpensive elements are vital. Among various alternative choices, sodium-ion batteries (NIBs) are promising because of plentiful resources and low costs of sodium metal. Different types of cathode materials for NIBs have been designed and studied to meet the challenging requirements. Among them pyrophosphate cathodes have shown promising electrochemical performance and thermal stability in sodium ion batteries (SIBs). In the present study, we report synthesis and thermal behavior of a novel $Na_2Fe_{0.33}Mn_{0.33}Co_{0.33}P_2O_7$ cathode material developed for sodium rechargeable batteries. The material was developed through solid state process. The structural analysis of $Na_2Fe_{0.33}Mn_{0.33}Co_{0.33}P_2O_7$ revealed that the substitution of multicomponent transition metals have achieved triclinic crystal structure (P1 space group). TGA/DTA and thermal in-situ XRD analyses (25~550^oC) confirm decent thermal stability of this material up to 550^oC even in the desodiated state with negligible weight loss (5%). Owing to its promising thermal stability, $Na_2Fe_{0.33}Mn_{0.33}Co_{0.33}P_2O_7$, would be an attractive cathode for sodium ion batteries.

Keywords: Sodium ion batteries, cathode material, thermal stability, in-situ analysis, multicomponent pyrophosphate

1. INTRODUCTION

Lithium-ion batteries (LIBs) [1-6] found applications ranging from portable electronics to electric vehicles. However, the cost of LIBs and scarcity of lithium reserves is yet a great concern for energy storage devices. Henceforth, replacement of LIBs [7-24] with sodium ion batteries (SIBs) [25~32] will significantly cut down the price of energy storage and usage. This is due to abundance of sodium reserves and their economic accessibility. In addition, Li ion replacement with Na ion will not require change of design in present LIBs, except change of cathode material (based on Na) and

respective electrolyte (e.g., $NaPF_6$ instead of $LiPF_6$) [33]. However, lower energy density and inferior kinetics, due to large size of Na ion, are the challenges to be addressed for sodium ion batteries. A variety of crystal structures for cathode materials have been explored to encounter problems for sodium ion batteries [34]. Previously, lithium poly-anions pyrophosphate material, $Li_2Fe_{0.5}Mn_{0.5}P_2O_7$ [35] exhibited better capacity than $Li_2MnP_2O_7$ within voltage range of 1.5~4.5V. During charging/discharging process, cyclic voltammogram showed wide oxidation peak for $Li_2Fe_{0.5}Mn_{0.5}P_2O_7$ ranging from 3.8~4.2V. The choice of transition metals [36-39] showed increment in operation voltage as well as activation of single phase A-insertion/extraction of Li or Na, due to its favorable kinetics during charge-discharge processes. Since the single phase processes have lower kinetic barrier, this mechanism is desirable for high power cell operations. As a comparison, in two phase reaction the nucleation and growth of second phase occurs in presence of concrete phase boundaries offering barrier to Li or Na diffusion kinetics. The optimization of operation parameters [40] and the formation of multicomponent systems (incorporation of more than one transition metal, *TM*) [35] not only lead to single phase mode but also tune the operation voltage for higher energy densities with an appropriate selection of TM. As an example, multicomponent olivine materials ($LiMPO_4$, M = *TM*s) exhibited higher cell potentials in comparison to the cell potentials for pure iron based olivine materials ($LiFePO_4$) [41-44].

As reported recently, both $Na_2FeP_2O_7$ and $Na_2MnP_2O_7$ concluded decent electrochemical performance and remarkable thermal stability as cathode materials for SIB [45, 46]. $Na_2FeP_2O_7$ exhibited reversible capacity of ~90 mAh/g, with triclinic framework in P1 space group and thermal stability of ~550^{o}C. Unlike Mn-based cathode materials having poor kinetics, [47-50] $Na_2MnP_2O_7$ also found a reversible capacity of ~90 mAh/g at 3.8V vs Na/Na^+ with 96% capacity retention after 30 cycles at scan rate of C/5. Henceforth, it was interesting to investigate the multicomponent effect in the family of sodium based pyrophosphate cathode materials. A multicomponent transition metals pyrophosphate cathode, $Na_2Fe_{0.33}Mn_{0.33}Co_{0.33}P_2O_7$, was developed through solid state synthesis process and its structural and thermal behaviors were studied. The novel $Na_2Fe_{0.33}Mn_{0.33}Co_{0.33}P_2O_7$ demonstrates decent thermal stability even in the desodiated state. The high thermal stability of $Na_2Fe_{0.33}Mn_{0.33}Co_{0.33}P_2O_7$ makes it attractive for sodium ion batteries. A detailed electrochemical behavior of $Na_2Fe_{0.33}Mn_{0.33}$ Co $_{0.33}P_2O_7$ will be reported separately.

2. EXPERIMENTAL

2.1 Material Synthesis

The stoichiometric amounts of precursors, Na_2CO_3 (Aldrich), $(NH_4)_2HPO_4$ (Aldrich), $MnC_2O_4.2H_2O$ (Aldrich), $FeC_2O_4.2H_2O$ (Aldrich) and $CoC_2O_4.2H_2O$ (Aldrich) were intimately mixed to synthesize $Na_2Fe_{0.33}Mn_{0.33}Co_{0.33}P_2O_7$ through solid state reaction. The mixed powder was pelletized and calcined under argon atmosphere at 350 ^{o}C for 3 hours. After calcination, pellets were cooled to room temperature (in Argon) and were grounded into fine powder. This powder was re-pelletized and

sintered at 600 ^{o}C for 6 hours under argon atmosphere to attain the desired phase, $Na_2Fe_{0.33}Mn_{0.33}Co_{0.33}P_2O_7$, according to the following chemical reaction.

$$Na_2CO_3 + 2(NH_4)_2HPO_4 + 1/3FeC_2O_4.2H_2O + 1/3MnC_2O_4.2H_2O + 1/3CoC_2O_4.2H_2O \rightarrow$$
$$Na_2Fe_{0.33}Mn_{0.33}\ Co_{0.33}P_2O_7 + 4H_2 + 2N_2 + 3CO + 7H_2O$$

The powder of desired phase was obtained after grinding the pellets that were cooled to room temperature under argon environment. Once the material was synthesized, it was coated with carbon to improve its electrical conductivity. The carbon coating was conducted in high energy ball mill with material to carbon (Active Material/Super P) ratio of 8:2 (wt. %). Silicon carbide balls were used for milling and the ball milling was carried out at 500 rpm for 24 hours. After ball milling, the carbon coated powder was pelletized and annealed at 600 ^{o}C for 10 hours under argon atmosphere to restore the crystallinity of the material.

2.2 Characterization

X-Ray Diffraction (XRD) measurements of the synthesized material were conducted by D/MAX-2500 XRD machine (Rigaku, Japan) to analyze the phase purity and crystal structure. Field Emission Scanning Electron Microscopy (FE-SEM) was used to study the size and morphology of pristine material and C-coated material by using XL30 FEG, Philips, and The Netherlands. The digested samples were prepared for ICP-MS (HP 4500) to measure the composition of pristine material ($Na_2Fe_{0.33}Mn_{0.33}Co_{0.33}P_2O_7$) and partially de-sodiated phase material, $Na_1Fe_{0.33}Mn_{0.33}Co_{0.33}P_2O_7$. FTIR spectrometer (JASCO, FR/IR-4100, Japan) was used to record the bond formation between the elements by KBr Pellet method in the range 1400~400. The weight loss with increase in temperature in Argon atmosphere was measured in Thermogravimetric Analysis (TGA) at heating rate of 10^{o}C/min and heat flow (exothermic/endothermic) was observed in Differential Thermal Analysis (DTA) at heating rate of 10^{o}C/min by using TG209 (NETZSCH, Germany).

2.3 Thermal in-situ XRD Characterization

Thermal in-situ analysis of pristine and partially de-sodiated materials were carried out using the aforementioned XRD machine. The de-sodiated samples were prepared as follows. Firstly, the pristine material was carbon coated as discussed earlier. Then the carbon-coated (C-coated) active material (75%w), carbon black (15%w) and polyvinylidene fluoride (PVDF) (10%w) were mixed in N-methyl-2-pyrrolidone (NMP) to form slurry. To homogenize, the slurry was stirred at 25˚C overnight and then cast onto the aluminum foil with doctor blade. The cast samples were dried at 110˚C for 2h under vacuum. The samples were then punched to the desired size to assemble the coin type half cells (CR2032). The coin cells were prepared, in argon filled glove box, by using Na thin disks, 1M sodium perchlorate ($NaClO_4$) in propylene carbonate (PC), and polyethylene separators (Celgard 2400) as the counter electrodes, electrolyte and separators, respectively. The partially de-sodiated samples ($NaFe_{0.33}Mn_{0.33}Co_{0.33}P_2O_7$) for thermal in-situ XRD analyses were prepared through electrochemical de-sodiation process. The cells were charged to 4.5 V, hold for two hours and then

immediately disassembled in the glove box. The electrodes were then thoroughly washed with propylene carbonate (PC). The cleaned samples were then dried at room temperature in the glove box. Thermal in-situ analyses of pristine and partially desodiated materials were carried out at heating rate of 5^{o}C/min, the dwell time between heating and measurement at each temperature was 3 min and the XRD scan rate of 1^{o}/min.

3. RESULTS AND DISCUSSION

3.1 Crystal Structure

The transition metals and synthesis parameters have significant influence on the polymorphic forms (crystal structures and space groups) of sodium metal pyrophosphates (*$Na_2MP_2O_7$, M = Fe, Mn, Co, Zn, Cu*). Although most of the pyrophosphate materials have different crystal structure they acquire open framework which facilitates Na-ions diffusion significantly during the battery operation. For instance, the crystal structure is tetragonal when the material is $Na_2ZnP_2O_7$ while the structure takes monoclinic crystal system when it is $Na_2CuP_2O_7$. $Na_2CoP_2O_7$ can adopt tetragonal (blue) crystal system or triclinic (rose) showing an allotropic behavior. The crystal structure of $Na_2CoP_2O_7$ depends on the synthesis, process parameters and choice of precursors. However, both $Na_2FeP_2O_7$ [45] and $Na_2MnP_2O_7$ [46] exhibit triclinic structure in space group P1.

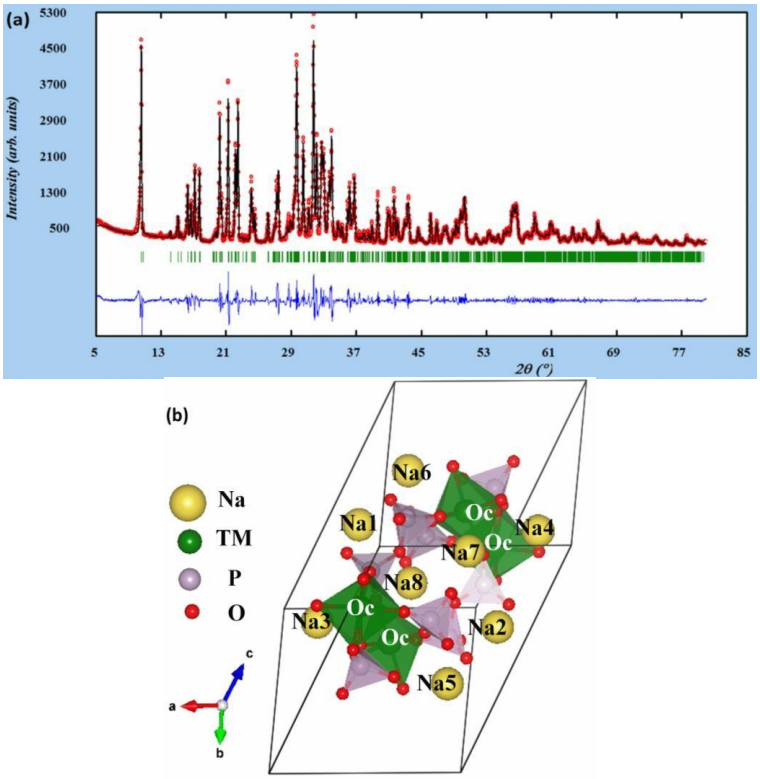

Figure 1. (a) XRD spectrum and pattern fitting of $Na_2Fe_{0.33}Mn_{0.33}Co_{0.33}P_2O_7$ (b) Crystal structure of triclinic $Na_2Fe_{0.33}Mn_{0.33}Co_{0.33}P_2O_7$

The XRD spectrum of $Na_2Fe_{0.33}Mn_{0.33}Co_{0.33}P_2O_7$ indicates that it adopts triclinic crystal structure with P1 space group. The Rietveld fitting of XRD spectrum of $Na_2Fe_{0.33}Mn_{0.33}Co_{0.33}P_2O_7$ presented in Figure 1(a) indicates that it is iso-structural with $Na_2FeP_2O_7$, $Na_2MnP_2O_7$ and $Na_2CoP_2O_7$-rose. The crystal structure of $Na_2Fe_{0.33}Mn_{0.33}Co_{0.33}P_2O_7$ can be presented by a framework comprising of the metal polyhedra (MO_6 and MO_5, M=Fe/Mn/Co) and the bridging pyrophosphate P_2O_7 groups [Figure 1(b)]. It can be noticed that corner sharing of all transition metal and phosphate polyhedra produces various channel structures for movement of Na ion. A unit cell consists of 8 Na sites (Na1–Na8) having different chemical and structural environments.

The XRD pattern (Figure 2) for pristine $Na_2Fe_{0.33}Mn_{0.33}Co_{0.33}P_2O_7$ and C-coated-annealed $Na_2Fe_{0.33}Mn_{0.33}Co_{0.33}P_2O_7$ validates that the pure phase is preserved after carbon coating and annealing processes because of matching of peaks of pristine and C-coated-annealed sample.

Figure 3 shows SEM images for both the pristine and C-coated-annealed $Na_2Fe_{0.33}Mn_{0.33}Co_{0.33}P_2O_7$. The inset of Figure 3(b) is TEM image of C-coated-annealed $Na_2Fe_{0.33}Mn_{0.33}Co_{0.33}P_2O_7$ which confirms the existence of carbon layer on the active material. The SEM image indicates that the average particle size is decreased after carbon coating due to ball milling.

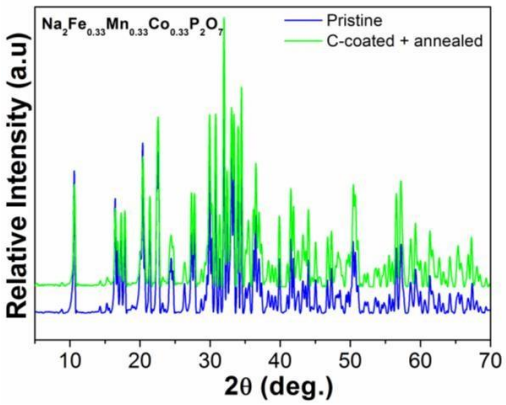

Figure 2. Powder XRD pattern for pristine and C-coated/annealed $Na_2Fe_{0.33}Mn_{0.33}Co_{0.33}P_2O_7$.

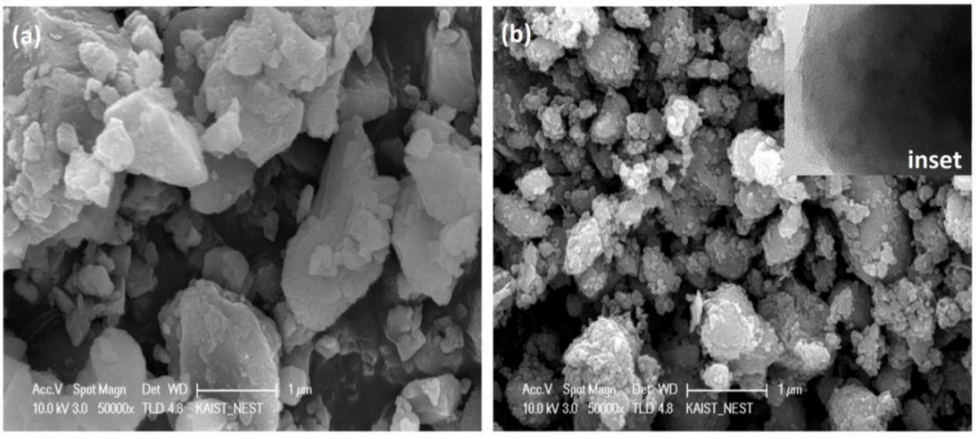

Figure 3. (a) SEM of pristine $Na_2Fe_{0.33}Mn_{0.33}Co_{0.33}P_2O_7$ (b) SEM of C-coated-annealed $Na_2Fe_{0.33}Mn_{0.33}Co_{0.33}P_2O_7$, inset is TEM showing carbon layer on $Na_2Fe_{0.33}Mn_{0.33}Co_{0.33}P_2O_7$

The phase purity of the synthesized material is also confirmed by ICP-MS and the compositional analysis is presented in Table 1. It can be noticed that the stoichiometric ratio of the synthesized compound is in good agreement with the targeted composition (Na:FeMnCo:P = 2.02:1.0:2.06).

Hence, XRD, SEM and ICP analyses validate the synthesis of phase pure $Na_2Fe_{0.33}Mn_{0.33}Co_{0.33}P_2O_7$ through solid state reaction.

Table 1. ICP composition analysis of $Na_2Fe_{0.33}Mn_{0.33}Co_{0.33}P_2O_7$.

Material	Element	Weight (%)	No. of Moles	Atomic (%)	At. Ratio
$Na_2Fe_{0.33}Mn_{0.33}Co_{0.33}P_2O_7$	Na	12.056	0.524	39.745	2.02
	Fe	4.909	0.088	6.649	1
	Mn	4.781	0.087	6.589	
	Co	5.021	0.085	6.452	
	P	16.585	0.535	40.564	2.06

The formation of pyrophosphate bonds were confirmed with Fourier transform infrared (FTIR) spectroscopy and the results are presented in Figure 4. The peak at band 738.3 and 909.6 cm^{-1} belonged to the symmetric and asymmetric vibrations, respectively, for P–O–P bonds in the pyrophosphate group. The existence of O–P–O vibrations between 492.4 and 601.8 cm^{-1} and P– O vibrations at 956 $cm^{-1}(v_{as})$ and 1153.7 $cm^{-1}(v_s)$ further confirms the formation of pure $Na_2Fe_{0.33}Mn_{0.33}Co_{0.33}P_2O_7$ via simple, solid state synthesis route.

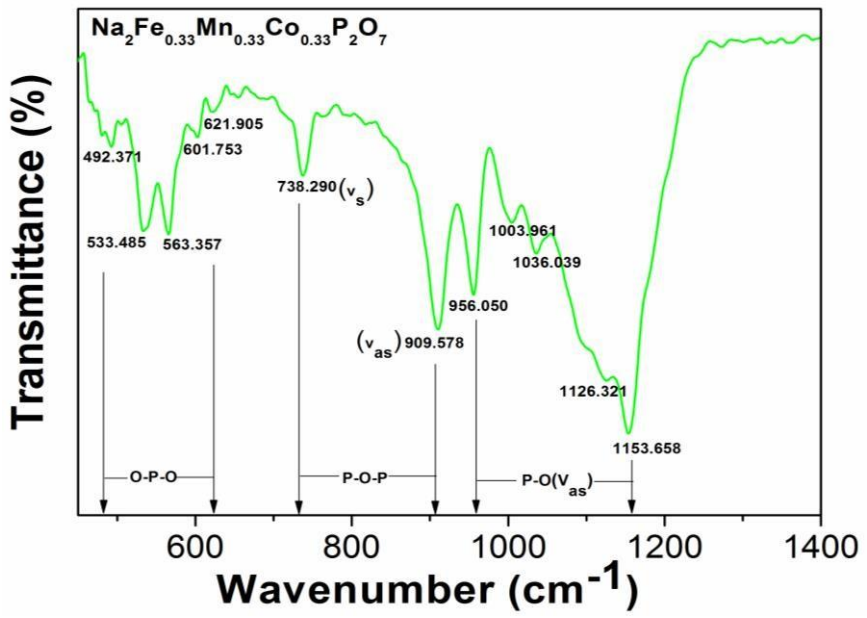

Figure 4. Fourier Transform Infrared Spectroscopy (FTIR) of triclinic $Na_2Fe_{0.33}Mn_{0.33}Co_{0.33}P_2O_7$

3.2 Thermal Stability

Similar to the case of $Na_2FeP_2O_7$ [45], negligible weight loss is observed for $Na_2Fe_{0.33}Mn_{0.33}Co_{0.33}P_2O_7$ when heated to a temperature of 550°C in argon atmosphere (Figure 5a). The exothermic peak at about 100°C is due to moisture evaporation. At the same time, decent thermal stability is also observed for partially desodiated material, $Na_1Fe_{0.33}Mn_{0.33}Co_{0.33}P_2O_7$ (Figure 5b).

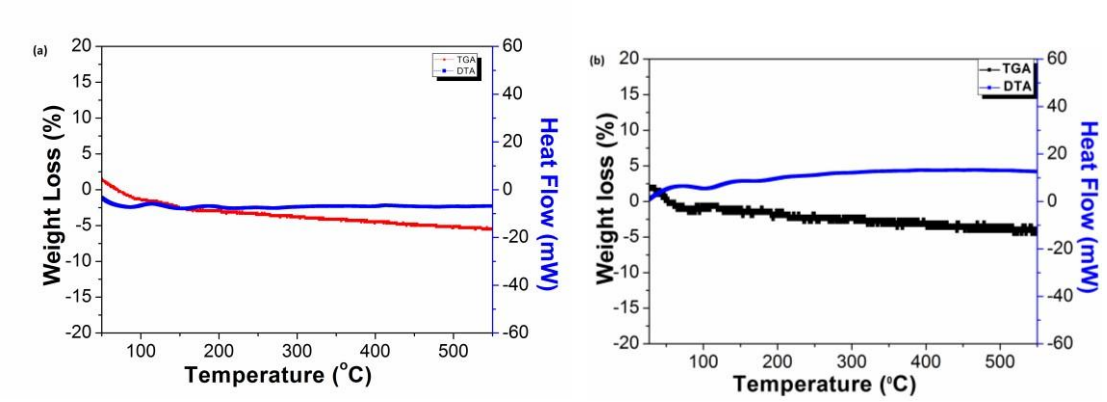

Figure 5. (a) TGA/DTA for $Na_2Fe_{0.33}Mn_{0.33}Co_{0.33}P_2O_7$ in Argon atmosphere at 10°C/min (b) TGA/DTA for $NaFe_{0.33}Mn_{0.33}Co_{0.33}P_2O_7$ in Argon atmosphere at 10°C/min.

As a comparison, the weight loss in $Na_2Fe_{0.33}Mn_{0.33}Co_{0.33}P_2O_7$ is comparable to the weight loss reported for $NaFeP_2O_7$ (2~5%) [45] and $LiFeP_2O_7$ (5%) [23]. Throughout temperature range (~550°C), no exothermic/endothermic peaks in the profile for differential thermal analysis (DTA) was noticed. DTA profile for partially desodiated state shows that thermal stability turns out to be similar to that of $NaFeP_2O_7$ [45] whereas superior to that of $LiFeP_2O_7$ in which an exothermic peak is appeared around 550°C [23].

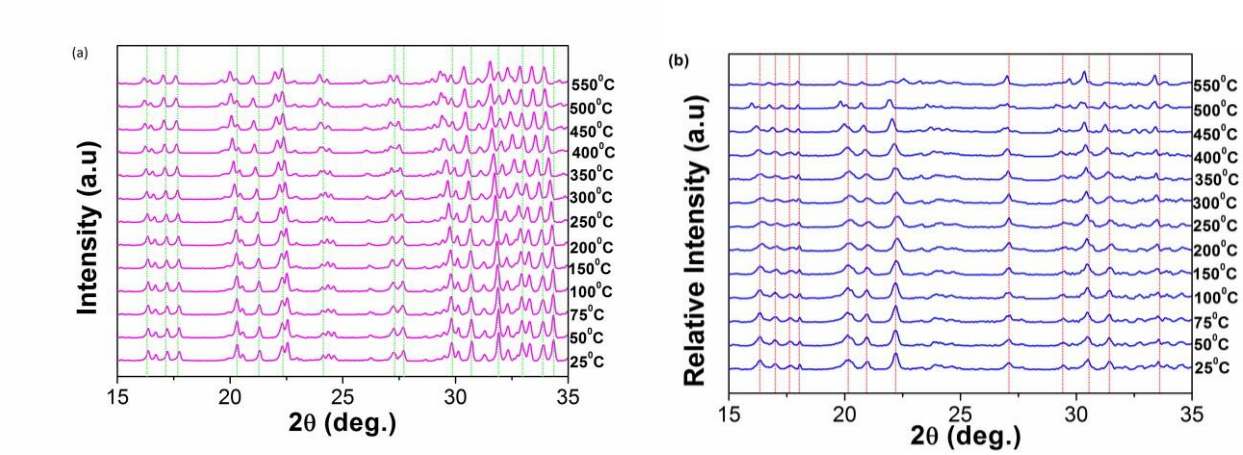

Figure 6. (a) In-situ thermal XRD pattern for $Na_2Fe_{0.33}Mn_{0.33}Co_{0.33}P_2O_7$ (b) In-situ thermal XRD pattern for $NaFe_{0.33}Mn_{0.33}Co_{0.33}P_2O_7$.

Further, the detailed thermal stability was observed by in-situ thermal XRD analysis. It can be noticed that there is not any phase transformation during thermal in-situ analysis of for

$Na_2Fe_{0.33}Mn_{0.33}Co_{0.33}P_2O_7$ up to 550^{o}C except unit cell expansion which is evidenced by the minor peak shifts to lower 2θ values at elevated temperature (Figure 6a). Similar behavior was recorded for partially desodiated sample, $NaFe_{0.33}Mn_{0.33}Co_{0.33}P_2O_7$, however, above 500^{o}C its phase changed and indexed to monoclinic ($P2_1/c$ space group) at 550^{o}C (Figure 6b).

Hence, it is found that multicomponent transition metals pyrophosphate cathode, $Na_2Fe_{0.33}Mn_{0.33}Co_{0.33}P_2O_7$, acquired excellent thermal stability similar to $Na_2FeP_2O_7$[45]. The promising thermal stability of $Na_2Fe_{0.33}Mn_{0.33}Co_{0.33}P_2O_7$ even in the desodiated state ($Na_1Fe_{0.33}Mn_{0.33}Co_{0.33}P_2O_7$) can be attributed to the solid-solution formation between the transition metals (Fe/Mn/Co) and its unique crystal structure.

4. CONCLUSION

A phase pure and well crystalline $Na_2Fe_{0.33}Mn_{0.33}Co_{0.33}P_2O_7$ has been synthesized through solid state reaction. The structural analysis confirms that the synthesized material adopts a triclinic crystal structure with P1 space group. The morphological analysis indicates that dry ball milling process is an effective way to form a carbon layer around the particles and to reduce the particle size. TGA/DTA and thermal in-situ XRD analyses confirm the decent thermal stability of $Na_2Fe_{0.33}Mn_{0.33}Co_{0.33}P_2O_7$ up to 500^{o}C even in the de-sodiated state ($Na_1Fe_{0.33}Mn_{0.33}Co_{0.33}P_2O_7$). The promising thermal stability of $Na_2Fe_{0.33}Mn_{0.33}Co_{0.33}P_2O_7$ makes them attractive for the development of safe sodium ion batteries.

ACKNOWLEDGEMENTS
This paper was made possible by NPRP grant # NPRP-5-569-2-232 from the Qatar National Research Fund (a member of Qatar Foundation). The statements made herein are solely the responsibility of the authors.

References

1. T. Nagaura, K. Tozawa, *Prog. Batteries Solar Cells*, 9 (1990) 209.
2. K. Mizushima, P.C. Jones, P.J. Wiseman, J.B. Goodenough, *Mater. Res. Bull.*, 15 (1980) 783.
3. M.M. Thackeray, W.I.F. David, P.G. Bruce, J.B. Goodenough, *Mater. Res. Bull.*, 18 (1983) 461.
4. J.R. Dahn, U. Sacken, M.W. Juzkow, H. J. Al-Janaby, *Electrochem. Soc.*, 138 (1991) 2207.
5. M. Armand , J. M. Tarascon , *Nature*, 451 (2008) 652.
6. H.-D. Lim, H. Park, H. Kim, J. Kim, B. Lee, Y. Bae, H. Gwon, K. Kang, *Angew. Chem. Int. Ed.*, 54 (2015) 9663.
7. J. Barker, M.Y. Saidi, J.L. Swoyer, *J. Electrochem. Soc.*, 150 (2003) A1394.
8. H.-J. Noh, J.W. Ju, Y.-K. Sun, *ChemSusChem*, 7 (2014) 245.
9. J. Barker, M.Y. Saidi, J.L. Swoyer, *J. Electrochem. Soc.*, 151 (2004) A1670.
10. R. Xu, J. C. M. Li, J. Lu, K. Amine, I. Belharouak, *J. Mater. Chem. A*, 3 (2015) 4170.
11. Y. Cui, A. Abouimrane, C.-J. Sun, Y. Ren, K. Ameen, *Chem. Commun.*50 (2014) 5576.
12. G. Tan, F. Wu, J. Lu, R. Chen, L. Li, K. Ameen, 6 (2014) 10611.
13. B.C. Melot, G. Rousse, J.N. Chotard, M. Ati, J. Rodriguez-Carvajal, M.C. Kemei, J.M. Tarascon, *Chem. Mater.*, 23 (2011) 2922.

14. M. Ati, M. T. Sougrati, N. Recham, P. Barpanda, J. B. Leriche, M. Courty, M. Armand, J. C. Jumas, J.M. Tarascon, *J. Electrochem. Soc.*, 157 (2010) A1007.
15. P. Barpanda, N. Recham, J. N. Chotard, K. Djellab, W. Walker, M. Armand, J.M. Tarascon, J. *Mater. Chem.*, 20 (2010) 1659.
16. R. Tripathi, G.R. Gardiner, M.S. Islam, L.F. Nazar, *Chem. Mater.*, 23 (2011) 2278.
17. R. Tripathi, T. N. Ramesh, B.L. Ellis, L.F. Nazar, *Angew. Chem.*, 49 (2010) 8738.
18. Y. Z. Dong, Y. M. Zhao, P. Fu, H. Zhou, X.M. Hou, *J. Alloys Compd.*, 461 (2008) 585.
19. A. Yamada, N. Iwane, Y. Harada, S. Nishimura, Y. Koyama, I. Tanaka, *Adv. Mater.*, 22 (2010) 3583.
20. H. Kim, S. Lee, Y-U. Park, H. Kim, J. Kim, S. Jeon, K. Kang, *Chem. Mater.*, 23 (2011) 3930.
21. H. Zhou, S. Upreti, N. A. Chernova, G. Hautier, G. Ceder, M.S. Whittingham, *Chem. Mater.*, 23 (2010) 293.
22. S. Nishimura, M. Nakamura, R. Natsui, A. Yamada, *J. Am. Chem. Soc.*, 132 (2010) 13596.
23. S. I. Nishimura, S. Hayase, R. Kanno, M. Yashima, N. Nakayama, A. Yamada, *J. Am. Chem Soc.*, 130 (2008) 13212.
24. A. Nyten, A. Abouimrane, M. Armand, T. Gustafsson, J.O. Thomas, *Electrochem. Commun.*, 7 (2005) 156.
25. S-W. Kim, D-H. Seo, X. Ma, G. Ceder, K. Kang, *Adv. Energy Mater.*, 2 (2012) 710.
26. J. Kim, D.-H. Seo, H. Kim, I. Park, J.-K. Yoo, S.-K. Jung, Y.-U. Park, W.A. Goddard III, K. Kang, *Energy Environ. Sci.*, 8 (2015) 540.
27. J.-Y. Hwang, S.-M. Oh, S.-T. Myung, K.Y. Chung, I. Belharouak, Y.-K. Sun, *Nat. Commun.*, 6 (2015) 7865.
28. D. Yuan, X. Hu, J. Qian, F. Pei, F. Wu, R. Mao, X. Ai, H. Yang, Y. Cao, *Electrochim. Acta*, 116 (2014) 300.
29. S.-M. Oh, S.-T. Myung, C. S. Yoon, J. Lu, J. Hassoun, B. Scrosati, K. Amine, Y.-K Sun, *Nano Lett.*, 14 (2014) 1620.
30. M. J. Brocker, J.M. L. Ho, G.M. Church, D. Soll, P.O'Donoghue, *Angew. Chem.*, 126 (2014) 1.
31. Y. Wang, L. Jue, R. Qiao, Z.-Z. Yang, S. Xu, X. Yu, L. Gu, Y.-S. Hu, W. Yang, K. Kang, H. Li, X.-Q Yang, L. Chen, X. Huang, *Nat. Commun.* 6 (2015) 359
32. H. Kim, J. Hong, K.-Y. Park, H. Kim, S.-W. Kim, K. Kim, *Chemical Reviews*, 114 (2014) 11788.
33. V. Palomares, P. Serras, I. Villaluenga, K.B. Hueso, J. Carretero-Gonzalez, T. Rojo, *Energy Environ. Sci.*, 5 (2012) 5884.
34. M.D. Slater, D. Kim, E. Lee, C.S. Johnson, *Adv. Funct. Mater.*, 23 (2012) 3255.
35. B.Dunn, H. Kamath, J.M. Tarascon, *Science*, 334 (2011) 928.
36. P. Senguttuvan, G. Rousse, V. Seznec, J-M. Tarascon, M.R. Palacin, *Chem. Mater.*, 23 (2011) 4109.
37. H. Zhou, S. Upreti, N.A. Chernova, G. Hautier, G. Ceder, M.S. Whittingham, *Chem. Mater.*, 23 (2011) 293.
38. P. Barpanda, M. Ati, B.C. Melot, G. Rousse, J.N. Chotard, M.L. Doublet, M.T. Sougrati, S.A. Corr, J.C. Jumas, J.M. Tarascon, *Nat. Mater.*, 10 (2011) 772.
39. D.H Seo, H. Gwon, S.W. Kim, J. Kim, K. Kang, *Chem. Mater.*, 22 (2009) 518.
40. H. Gwon, D.H Seo, S.W. Kim, J. Kim, K. Kang, *Adv. Func. Mater.*, 19 (2009) 3285.
41. T. Muraliganth, A.J. Manthiram, *Phys. Chem. C*, 114 (2010) 15530.
42. X. Wu, J. Zheng, Z. Gong, Y.J. Yang, *Mater. Chem.*, 21 (2011) 18630.
43. N.N. Bramnik, K.G. Bramnik, K. Nikolowski, M. Hinterstein, C. Baehtz, H. Ehrenberg, Electrochem. *Solid State Lett.*, 8 (2005) A379.
44. H.T. Kuo, T.S. Chan, N.C. Bagkar, G.Q. Liu, R.S. Liu, C.H. Shen, A.S. Shy, X.K. Xing, J.M. Chen, *J. Phys. Chem. B*, 112 (2008) 8017.
45. Park, Y. U.; Kim, J.; Gwon, H.; Seo, D. H.; Kim, S. W.; Kang, K. *Chem. Mater.*, 22 (2010) 2573.

46. Wang, X. J.; Yu, X. Q.; Li, H.; Yang, X. Q.; McBreen, J.; Huang, X. *J. Electrochem. Commun.*, 10 (2008) 1347.
47. H. Kim, R.A. Shakoor, C.S. Park, S.Y. Lim, J-S Kim, Y. N. Jo, W. Cho, K. Miyasaka, R. Kahraman, Y. Jung, J.W. Choi, *Adv. Funct. Mater.*, 23 (2013) 1147.
48. C.S. Park, H. Kim, R.A. Shakoor, E. Yang, S.Y. Lim, R. Kahraman, Y. Jung, J.W. Choi, *J. Am. Chem. Soc.*, 135 (2013) 2787.
49. Zhou, H.; Upreti, S.; Chernova, N. a.; Hautier, G.; Ceder, G.; Whittingham, M. S. *Chem. Mater.*, 23 (2011) 293.
50. Tamaru, M.; Barpanda, P.; Yamada, Y.; Nishimura, S.-i.; Yamada, A. J. *Mater. Chem.*, 22 (2012) 24526.
51. N. Furuta, S. Nishimura, P. Barpanda, A. Yamada, *Chem. Mater.*, 24 (2012) 1055.
52. S. P. Ong, V. L. Chevrier, G. Ceder, *Phys. Rev. B*, 83 (2011) 075112.